symmetry

Article

Further Stability Criteria for Sampled-Data-Based Dynamic Positioning Ships Using Takagi–Sugeno Fuzzy Models

Minjie Zheng, Yulai Su and Changjian Yan *

Navigation College, Jimei University, Xiamen 361021, China; mjzheng@jmu.edu.cn (M.Z.); suyulai1128@163.com (Y.S.)
* Correspondence: chjyan@jmu.edu.cn

Abstract: This article discusses the stability problem of sampled-data-based dynamic positioning ships (DPSs) using Takagi–Sugeno (T-S) fuzzy models. Firstly, dynamic equations for sampled-data DPSs are established. Simultaneously combining several symmetric matrices with new integral terms, a novel Lyapunov–Krasovskii function (LKF) is constructed, which allows the information of a sampling pattern to be fully captured. Next, via the constructed LKF, the positive definiteness requirements of a LKF are further relaxed, and the conservatism of the result can be reduced. Consequently, stability criteria are given, and fuzzy sampled-data controllers are designed in terms of linear matrix inequality (LMI). Finally, a simulation example is provided to verify the superiority and applicability of the developed methods.

Keywords: fuzzy system; dynamic positioning ship; sampled-data control; Lyapunov–Krasovskii functional; Takagi−Sugeno fuzzy models

check for updates

Citation: Zheng, M.; Su, Y.; Yan, C. Further Stability Criteria for Sampled-Data-Based Dynamic Positioning Ships Using Takagi–Sugeno Fuzzy Models. *Symmetry* **2024**, *16*, 108. https://doi.org/10.3390/sym16010108

Academic Editor: Hsien-Chung Wu

Received: 27 November 2023
Revised: 13 January 2024
Accepted: 14 January 2024
Published: 16 January 2024

1. Introduction

A DPS is a system that utilizes a combination of computers, position reference systems, and thrusters to maintain a ship at a predetermined position [1]. It uses the measurement equipment of the ship to collect environmental parameters, calculates the thrust of the thruster based on the parameters of the global positioning system, and maintains fixed positions and headings. Compared with anchoring positioning, a DPS relies only on ship thrusters to overcome environmental interference and achieves the desired position for engineering operations. Therefore, it has unique advantages, such as infinite depth operation, high mobility, and precise positioning. And a DPS has a wide range of applications, such as cargo supply, oil extraction, heavy lifting, ocean surveying, deep water exploration, ocean rescue, etc. Therefore, more and more scholars are studying the control problem of DPSs ([2–7]). For example, reference [2] conducted fuzzy modeling for a DPS based on the range of the yaw angle, and designed an observer that can provide excellent DP performances that reduces the negative impact of external disturbance. Reference [3] designed a quantization controller based on a switching mechanism to ensure the robustness and control performance of a DPS, and signal quantization, time delay, and thruster failure were simultaneously considered. Reference [4] used a neural network to design a system controller for a DPS, and auxiliary devices like thruster and tug were considered. Reference [5] proposed a multitask control system for a DPS by introducing the integrated neural controller, and the neural network structures were not required to be retrained while performing different tasks. Reference [6] combined Luenberger observer and odd–even space technology to DPS detect thruster faults, and designed a reconfigurable variable structure controller to achieve fault-tolerant targets.

Recently, digital devices have been gradually replacing continuous time devices in actual industrial systems. These control systems, which include continuous time objects and discrete time controllers, are considered sampled-data control systems. Compared with traditional continuous time control systems, sampled-data control systems only require the instantaneous sampling information of the system state, and thus greatly reduce information transmission and communication costs. Therefore, they are widely applicable in various systems, such as multiagent systems [8,9], chaotic systems [10,11], master–slave systems [12], neural networks systems [13,14], Markovian jump systems [15], time delay systems [16,17], etc. They have also been used in severable practical engineering applications, including high-speed trains [18], autonomous airships [19], multipurpose supply vessels [20], luxury cruises [21], unmanned marine vehicles [22], etc. For example, reference [23] studied a discrete sampled-data system with a saturated actuator, and designed a robust controller using a convex approach to ensure the local stability of the systems with interval time delays. Reference [24] creatively introduced an algorithm for event-triggered sampling control and proposed intermittent triggering conditions at fixed sampling times. Reference [25] focused on a class of multi-agent systems and transformed them into discrete systems, analyzed the inherent relationship between the sampling period and steady-state performance, and obtained the range of the sampling period. Reference [26] investigated the mean square exponential stability problem of a sampled-data resistive memory neural network (MNN) system. The concept of security level was first proposed to measure the anti-attack capability of a MNN. Reference [27] proposed a dual deep Q-network method to solve the sampled-data control problem of PBCNs, and an optimal sampled-data controller was designed to stabilize the PBCN.

Nowadays, T-S fuzzy systems (TSFSs) have obtained wide attention [28], and severable sampled-data control results have been reported for TSFSs. Reference [29] investigated the adaptive static output control problem of TSFSs with uncertainties. To reduce the sampled-data frequency, new adaptive memory event-triggering mechanisms were proposed. Reference [30] investigated the quantitative sampled-data control issue of a network TSFS using a random network attack, and then new time delay product relaxation conditions were proposed. Reference [31] proposed a non-periodic event-triggered communication scheme to solve the exponential stabilization issue of TSFSs under non-periodic sampling conditions. Reference [32] investigated the stability problem of TSFSs under sampled-data control using a new asymmetric LKF. Cyclic and discontinuous function terms were improved by combining time delay and each sampling interval. Reference [33] investigated the stability characteristics of a TSFS under sampled-data control. Based on the input delay method, the system was converted to a variable time-delay system. Using the reciprocally convex combination approach, stability criteria were established to guarantee the stability of the TSFS.

A DPS is a sampled-data control system that uses a computer to collect severable sensor information, and then the sailing status of the ship is obtained [34]. Recently, many sampled-data control achievements of DPSs have been reported. In [35], the trajectory tracking problem of a nonlinear sampled-data DPS was considered, and a reduced order observer was introduced using the Euler approximation model. In [36], the systems of the sampled-data DPS were converted into neutral systems; then the Wirtinger integral inequality and delay-decomposition methods were introduced to reduce the conservatism of the system. In [37], the fault-tolerant control problem of a sampled-data DPS was studied using actuator failure. Reference [38] established fuzzy models for a sampled-data DPS, and convex reciprocal inequalities were used to obtain the stability condition. Reference [39] investigated the non-periodic sampling tracking control problem of a DPS using actuator faults, and by introducing a new LKF, the mean square exponential stability criterion was obtained.

However, there is still room for improvement regarding the sampling control problem of DPSs. Firstly, during the LKF construction process, some terms in a LKF share common quadratic functions. Secondly, some available information for sampling patterns is completely ignored. Thirdly, conditions on LKFs are too strict; that is, some matrices in a single Lyapunov are strictly positive definite. To some extent, these limitations lead to a decrease in the conservatism of the results.

Motivated by the above analysis, the fuzzy sampling control problem of a nonlinear DPS is studied here. Firstly, the dynamic equations of the system are established. Secondly, an improved LKF is established to fully capture the characteristics of sampling modes and further relax the positive definiteness requirements of LKFs. Based on the LMIs, stability conditions are derived, and the designed approach of the sampling controller is given. Finally, the superiority of this method is verified through a simulation example.

The developments and novelty of this article are summarized as follows.

(1) By introducing some novel terms, like $d(t)\int_{-d(t)}^{0}\int_{t+\theta}^{t}\dot{x}(s)^{T}Z\dot{x}(s)dsd\theta$, in the LKF, the available characteristics of sampling patterns have been fully captured.

(2) Compared with the LKF in existing results, more available matrices are effectively used in the LKF. Therefore, the proposed LKF has a more general form.

(3) Compared with the existing results, X-dependent terms are introduced in the LKF, which are not required to be positive definite, and this means that the limitation conditions of the symmetric matrices are overcome.

Notations: $\mathbb{R}^m$ is m-dimensional Euclidean space, M^T is the transpose of matrix M, "*" is the symmetric term of a matrix, and $\|\cdot\|$ is the spectral norm in $\mathbb{R}^m$.

The subsequent structure of this article is as follows. In Section 2, models of the sampled-data DPS system are established. In Section 3, the main results are described. In Section 4, numerical validation and comparison results are described.

2. Problem Formulation

In order to deal with the sampled-data control problem for DPSs, dynamic equations for a DPS are considered:

$$\begin{aligned} &M\dot{v}(t)+Dv(t)+G\eta(t)=u(t),\\ &\dot{\eta}(t)=J(\psi(t))v(t), \end{aligned} \tag{1}$$

where

$$M=\begin{bmatrix} m-X_{\dot{u}} & 0 & 0\\ 0 & m-Y_{\dot{v}} & mx_G-Y_{\dot{r}}\\ 0 & mx_G-Y_{\dot{r}} & I_z-N_{\dot{r}} \end{bmatrix},\ D=\begin{bmatrix} -X_{\dot{u}} & 0 & 0\\ 0 & -Y_{\dot{v}} & -Y_{\dot{r}}\\ 0 & -Y_{\dot{r}} & -N_{\dot{r}} \end{bmatrix},$$

$$J(\psi(t))=\begin{bmatrix} \cos(\psi(t)) & -\sin(\psi(t)) & 0\\ \sin(\psi(t)) & \cos(\psi(t)) & 0\\ 0 & 0 & 1 \end{bmatrix}.$$

where $\eta(t)=\begin{bmatrix} x_a(t) & y_a(t) & \psi(t)\end{bmatrix}^T$ is the position vector in the northeast coordinate system; $x_a(t)$ and $y_a(t)$ represent the x and y positions, respectively; and $\psi(t)$ represents the yaw angle. $v(t)=\begin{bmatrix} p(t) & v(t) & r(t)\end{bmatrix}^T$ denotes the velocity vector in the attached coordinate system (see Figure 1). $p(t)$ is surge velocity; $v(t)$ is sway velocity; and $r(t)$ is yaw velocity. $J(\psi)$ represents the rotation matrix of the two coordinates. $u(t)$ is the control force vector; and M and D are the inertial matrix and damping matrix, respectively. $G=diag\{g_{11},g_{22},g_{33}\}$ represents the mooring force matrix. m is the ship's mass; I_z is the moment of inertia; x_G is the distance vector; and $X_{\dot{u}}$, $Y_{\dot{v}}$, $N_{\dot{r}}$ $Y_{\dot{r}}$ are the added mass.

Remark 1. *The derivation of the ship model is based on [1]. The case study in this paper is a dynamic positioning ship controlled by thrusters. The damping force is assumed to be linear because the ship's speed is slow. Therefore, dynamic equations for surge, sway, and yaw for the DPS are considered in this paper.*

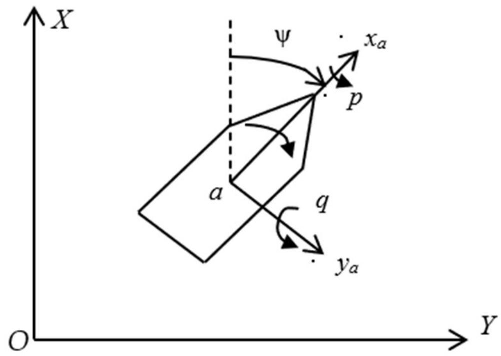

Figure 1. Body-fixed coordinate systems.

Define

$$\begin{aligned} x(t) &= \begin{bmatrix} \eta(t) & v(t) \end{bmatrix}^T \\ &= \begin{bmatrix} x_a(t) & y_a(t) & \psi(t) & p(t) & q(t) & r(t) \end{bmatrix}^T, \end{aligned} \tag{2}$$

and let

$$-M^{-1}D = \begin{bmatrix} a_{11} & 0 & 0 \\ 0 & a_{22} & a_{23} \\ 0 & a_{32} & a_{33} \end{bmatrix}, M^{-1} = \begin{bmatrix} d_{11} & 0 & 0 \\ 0 & d_{22} & d_{23} \\ 0 & d_{32} & d_{33} \end{bmatrix}, -M^{-1}G = \begin{bmatrix} b_{11} & 0 & 0 \\ 0 & b_{22} & b_{23} \\ 0 & b_{32} & b_{33} \end{bmatrix}. \tag{3}$$

where $a_{11}, a_{22}, a_{23}, a_{32}, a_{33}, d_{11}, d_{22}, d_{23}, d_{32}, d_{33}, b_{11}, b_{22}, b_{23}, b_{32}, b_{33}$ are constant.

Substitute (2) and (3) into (1) that

$$\dot{x}(t) = A(t)x(t) + Bu(t), \tag{4}$$

where

$$A(t) = \begin{bmatrix} 0 & 0 & 0 & \cos(\psi(t)) & -\sin(\psi(t)) & 0 \\ 0 & 0 & 0 & \sin(\psi(t)) & \cos(\psi(t)) & 0 \\ 0 & 0 & 0 & 0 & 0 & 1 \\ b_{11} & 0 & 0 & a_{11} & 0 & 0 \\ 0 & b_{22} & b_{23} & 0 & a_{22} & a_{23} \\ 0 & b_{32} & b_{33} & 0 & a_{32} & a_{33} \end{bmatrix}, B = \begin{bmatrix} 0 & 0 & 0 \\ 0 & 0 & 0 \\ 0 & 0 & 0 \\ d_{11} & 0 & 0 \\ 0 & d_{22} & d_{23} \\ 0 & d_{32} & d_{33} \end{bmatrix}.$$

The overall fuzzy model is obtained that

Mode Rule i: IF $z_1(t)$ is f_{i1}, $\cdots z_n(t)$ is f_{in}, THEN

$$\dot{x}(t) = A_i x(t) + B_i u(t),\ i = 1, 2, \ldots, n \tag{5}$$

where $z_1(t), z_2(t), \ldots, z_{\mathrm{n}}(t)$ denote premise variables, f_{ij} denotes the fuzzy set, and n denotes the rules number.

Assume the yaw angle satisfies $\psi(t) \in (-\pi/2, \pi/2)$, then T-S fuzzy rules are considered that

Model Rule 1:

IF $\psi(t)$ is about 0

Then

$$\dot{x}(t) = A_1 x(t) + B_1 u(t), \tag{6}$$

Model Rule 2:

IF $\psi(t)$ is about $\frac{\pi}{2}\left(\psi(t) < \frac{\pi}{2}\right)$

Then

$$\dot{x}(t) = A_2 x(t) + B_2 u(t), \tag{7}$$

Model Rule 3:
IF $\psi(t)$ is about $-\frac{\pi}{2}\left(\psi(t) < \frac{\pi}{2}\right)$
Then

$$\dot{x}(t) = A_3 x(t) + B_3 u(t), \tag{8}$$

where

$$A_1 = \begin{bmatrix} 0 & 0 & 0 & 1 & -\alpha & 0 \\ 0 & 0 & 0 & \alpha & 1 & 0 \\ 0 & 0 & 0 & 0 & 0 & 1 \\ b_{11} & 0 & 0 & a_{11} & 0 & 0 \\ 0 & b_{22} & b_{23} & 0 & a_{22} & a_{23} \\ 0 & b_{32} & b_{33} & 0 & a_{32} & a_{33} \end{bmatrix}, A_2 = \begin{bmatrix} 0 & 0 & 0 & \beta & -1 & 0 \\ 0 & 0 & 0 & 1 & \beta & 0 \\ 0 & 0 & 0 & 0 & 0 & 1 \\ b_{11} & 0 & 0 & a_{11} & 0 & 0 \\ 0 & b_{22} & b_{23} & 0 & a_{22} & a_{23} \\ 0 & b_{32} & b_{33} & 0 & a_{32} & a_{33} \end{bmatrix},$$

$$A_3 = \begin{bmatrix} 0 & 0 & 0 & \beta & 1 & 0 \\ 0 & 0 & 0 & -1 & \beta & 0 \\ 0 & 0 & 0 & 0 & 0 & 1 \\ b_{11} & 0 & 0 & a_{11} & 0 & 0 \\ 0 & b_{22} & b_{23} & 0 & a_{22} & a_{23} \\ 0 & b_{32} & b_{33} & 0 & a_{32} & a_{33} \end{bmatrix}, B_i = \begin{bmatrix} 0 & 0 & 0 \\ 0 & 0 & 0 \\ 0 & 0 & 0 \\ d_{11} & 0 & 0 \\ 0 & d_{22} & d_{23} \\ 0 & d_{32} & d_{33} \end{bmatrix}, \ i = 1, 2, 3.$$

and in which $\alpha = \sin(2^\circ)$ and $\beta = \cos(88^\circ)$. The overall T-S fuzzy model is obtained that

$$\dot{x}(t) = \sum_{i=1}^{3} \mu_i(z(t))[A_i x(t) + B_i u(t)], \tag{9}$$

where

$$\begin{aligned} &\mu_i(z(t)) = \frac{\omega_i(z(t))}{\sum_{i=1}^{3} \omega_i(z(t))} \geq 0, \ i = 1, 2, 3, \\ &\omega_i(z(t)) = \prod_{j=1}^{n} f_{ij}(z_j(t)), \\ &\sum_{i=1}^{3} \mu_i(z(t)) = 1, \\ &z(t) = [z_1(t), z_2(t), \ldots, z_n(t)], \end{aligned}$$

and in which $f_{ij}(z_j(t))$ denotes the membership grade of $z_j(t)$. The membership function of $\psi(t)$ is shown in Figure 2.

A diagram of the fuzzy modeling and controller design is shown in Figure 3.

Assume measurement signals of the DPS are available at the sampling time, which satisfies that $0 = t_0 < t_1 < \cdots < t_k < \cdots < \lim_{k \to \infty} t_k = +\infty$.

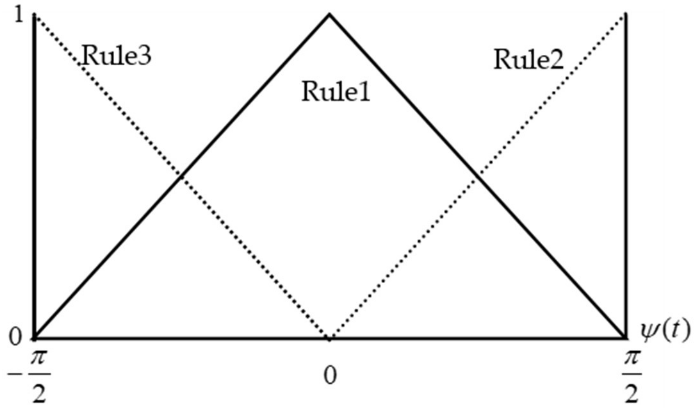

Figure 2. Membership function of $\psi(t)$.

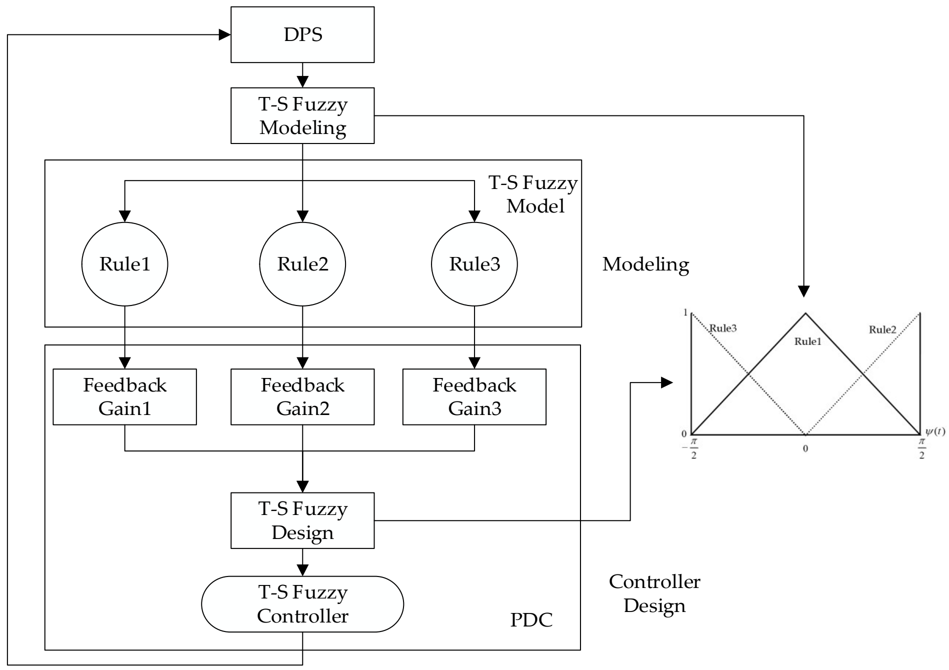

Figure 3. Fuzzy modeling and controller design.

The sampling interval is supposed as

$$t_{k+1} - t_k \leq d, \forall k \geq 0, d > 0,$$

where d denotes the upper bound of the sampling interval. Next, the corresponding sampled-data controller is considered

$$u(t) = Kx(t_k),\ t_k \leq t < t_{k+1}, \tag{10}$$

where K denotes the gain matrix. Next, T-S fuzzy controllers are expressed that

Controller Rule 1:
IF $\psi(t)$ is about 0
Then

$$u(t) = K_1 x(t_k). \tag{11}$$

Controller Rule 2:
IF $\psi(t)$ is about $\frac{\pi}{2}\left(\psi(t) < \frac{\pi}{2}\right)$
Then

$$u(t) = K_2 x(t_k). \tag{12}$$

Controller Rule 3:
IF $\psi(t)$ is about $-\frac{\pi}{2}\left(\psi(t) < \frac{\pi}{2}\right)$
Then

$$u(t) = K_3 x(t_k). \tag{13}$$

Next, the following fuzzy controller is obtained

$$u(t) = \sum_{j=1}^{3} \mu_j(z(t)) K_j x(t_k), t_k \le t < t_{k+1}, k = 0, 1, 2, \ldots \tag{14}$$

Substitute (14) into (11) to obtain

$$\dot{x}(t) = \sum_{i=1}^{3} \sum_{j=1}^{3} \mu_i(z(t)) \mu_j(z(t)) \left[A_i x(t) + B_i K_j x(t_k)\right] \tag{15}$$

For the further deriving process, the lemma is given as:

Lemma 1 ([40]). *For given matrix $Z \in \mathbb{R}^n, Z > 0$, scalars $\tau_2 > \tau_1$, vector function $w : [\tau_1, \tau_2] \in R^n$, the following inequality holds*

$$\begin{aligned} &-\int_{t-\tau_2}^{t-\tau_1} w^T(\alpha) Z w(\alpha) d\alpha \\ &\le -\tfrac{1}{\tau_2-\tau_1}\left(\int_{t-\tau_2}^{t-\tau_1} w^T(\alpha) d\alpha\right)^T Z \left(\int_{t-\tau_2}^{t-\tau_1} w(\alpha) d\alpha\right) \end{aligned} \tag{16}$$

$$\begin{aligned} &-\int_{-\tau_2}^{-\tau_1} \int_{t+\alpha}^{t} w^T(s) Z w(s) ds d\alpha \\ &\le -\tfrac{2}{\tau_2^2-\tau_1^2}\left(\int_{-\tau_2}^{-\tau_1} \int_{t+\alpha}^{t} w^T(s) ds d\alpha\right)^T Z \left(\int_{-\tau_2}^{-\tau_1} \int_{t+\alpha}^{t} w(s) ds d\alpha\right) \end{aligned} \tag{17}$$

3. Main Results

In this section, by constructing an appropriate LKF, the stability conditions of system (15) are given.

3.1. Construction of the Lyapunov Function

Firstly, the notations are defined as follows:

$$\begin{aligned} &\tau(t) = t - t_k,\ d(t) = d - \tau(t), \\ &\varsigma(t) = \begin{bmatrix} x^T(t) & x^T(t_k) & \int_{t_k}^{t} x^T(s) ds \end{bmatrix}^T \\ &\zeta(t) = \begin{bmatrix} x^T(t) & \dot{x}(t)^T & x^T(t_k) & \int_{t_k}^{t} x^T(s) ds \end{bmatrix} \end{aligned}$$

Theorem 1. *The system (15) is asymptotically stable, if there exist symmetric matrices $P > 0$, $Q > 0$, $Z > 0$, $\begin{bmatrix} R_{11} & R_{12} \\ * & R_{22} \end{bmatrix} > 0$, $\begin{bmatrix} U_{11} & U_{12} \\ * & U_{22} \end{bmatrix} > 0$, $X_{11}, X_{13}, X_{22}, X_{23}, X_{33}, G$, $M_{ij} = \begin{bmatrix} M_{1ij}^T & M_{2ij}^T & M_{3ij}^T & M_{4ij}^T \end{bmatrix}^T$, $N_{ij} = \begin{bmatrix} N_{1ij}^T & N_{2ij}^T & N_{3ij}^T & N_{4ij}^T \end{bmatrix}^T$ and scales $d > 0$, $\varepsilon_i, i = 1, 2, 3, 4$, such that*

$$\Psi_1^{ij} = \begin{bmatrix} P + d\left(X_{11} + X_{11}^T + Q\right) & d\left(X_{11} + X_{22} - Q\right) & dX_{13} \\ * & d\left(X_{11} + X_{22}^T + Q\right) & dX_{23} \\ * & * & dX_{33} \end{bmatrix} > 0 \tag{18}$$

$$\Psi_2^{ij} = \begin{bmatrix} \Xi_{11}^{ij} + \Omega_{11}^{ij} & \Xi_{12}^{ij} + \Omega_{12}^{ij} & \Xi_{13}^{ij} + \Omega_{13}^{ij} & \Xi_{14}^{ij} + dX_{33}^T \\ * & \Xi_{22}^{ij} + \Omega_{22}^{ij} & \Xi_{23}^{ij} + \Omega_{23}^{ij} & \Xi_{11}^{ij} + dX_{13} \\ * & * & \Xi_{33}^{ij} + \Omega_{33}^{ij} & \Xi_{34}^{ij} \\ * & * & * & \Xi_{44}^{ij} \end{bmatrix} < 0 \tag{19}$$

$$\Psi_3^{ij} == \begin{bmatrix} \Pi_{11ij} & \Pi_{12ij} \\ * & \Pi_{22} \end{bmatrix} < 0. \tag{20}$$

where

$$\Pi_{11ij} = \begin{bmatrix} \Xi_{11}^{ij} + \Omega_{11}^{ij} & \Xi_{12}^{ij} + dN_{2ij}^T & \Xi_{13}^{ij} + dN_{3ij}^T & \Xi_{14}^{ij} + dN_{4ij}^T \\ * & \Xi_{22}^{ij} + \frac{d^2}{4}Z & \Xi_{23}^{ij} & \Xi_{24}^{ij} \\ * & * & \Xi_{33}^{ij} + \Omega_{33}^{ij} & \Xi_{34}^{ij} \\ * & * & * & \Xi_{44}^{ij} \end{bmatrix},$$

$$\Pi_{12ij} = \begin{bmatrix} -dM_{1ij} & dN_{1ij} \\ -dM_{2ij} & dN_{2ij} \\ -dE^T R_{12}^T - dM_{3ij} & dN_{3ij} \\ -dM_{4ij} & dN_{4ij} \end{bmatrix},$$

$$\Pi_{22} = \begin{bmatrix} -dQ - dR_{11} & 0 \\ * & -2Z \end{bmatrix},$$

$$\Xi_{11}^{ij} = -\left(X_{11} + X_{11}^T\right) + M_{1ij}^T + M_{1ij} + \varepsilon_1 A_i G^T + \varepsilon_1 G A_i^T$$
$$\Xi_{12}^{ij} = P + M_{2ij}^T - \varepsilon_1 G - \varepsilon_2 A_i^T G^T$$
$$\Xi_{13}^{ij} = (X_{11} + X_{22}) + M_{3ij}^T - M_{1ij} + \varepsilon_1 G B_i K_j + \varepsilon_3 A_i^T G^T$$
$$\Xi_{14}^{ij} = -X_{13} + M_{4ij}^T - N_{1ij} + \varepsilon_4 A_i^T G^T$$
$$\Xi_{22}^{ij} = -\varepsilon_2 G - \varepsilon_2 G^T$$
$$\Xi_{23}^{ij} = -M_{2ij} + \varepsilon_2 G B_i K_j - \varepsilon_3 G^T$$
$$\Xi_{24}^{ij} = -\varepsilon_4 G^T - N_{2ij}$$
$$\Xi_{33}^{ij} = -\left(X_{22} + X_{22}^T\right) - M_{3ij}^T - M_{3ij} + \varepsilon_3 G B_i K_j + \varepsilon_3 K_j^T B_i^T G^T$$
$$\Xi_{34}^{ij} = -X_{23} - U_{12} - M_{4ij}^T - N_{3ij} + \varepsilon_4 K_j^T B_i^T G^T$$
$$\Xi_{44}^{ij} = -X_{33} - \frac{1}{d} U_{22} - N_{4ij}^T - N_{4ij}$$
$$\Omega_{11} = d\left(X_{13} + X_{13}^T\right) + dU_{22} - Z$$
$$\Omega_{12} = dX_{11} + dX_{11}^T$$
$$\Omega_{13} = dX_{23}^T + dU_{12}^T + Z$$
$$\Omega_{22} = dR_{11} + dQ + \frac{d^2}{4} Z$$
$$\Omega_{23} = -d(X_{11} + X_{22}) + dR_{12}$$
$$\Omega_{33} = dR_{22} + dU_{11} - Z$$

Proof. Consider the following LKF

$$V(t) = \sum_{i=1}^{4} V_i(t),\ t \in [t_k, t_{k+1}) \tag{21}$$

$$V_1(t) = x(t)^T P x(t) + d(t)\varsigma(t)^T X \varsigma(t) + d(t)\int_{t_k}^{t} \dot{x}(s)^T Q \dot{x}(s) ds$$
$$V_2(t) = d(t)\int_{t_k}^{t} \begin{bmatrix} \dot{x}(s) \\ x(t_k) \end{bmatrix}^T R \begin{bmatrix} \dot{x}(s) \\ x(t_k) \end{bmatrix} ds$$
$$V_3(t) = d(t)\int_{t_k}^{t} \begin{bmatrix} x(t_k) \\ x(s) \end{bmatrix}^T U \begin{bmatrix} x(t_k) \\ x(s) \end{bmatrix} ds$$
$$V_4(t) = d(t)\int_{-d(t)}^{0} \int_{t+\theta}^{t} \dot{x}(s)^T Z \dot{x}(s) ds d\theta$$

where

$$X = \begin{bmatrix} X_{11} + X_{11}^T & -X_{11} - X_{22} & X_{13} \\ * & X_{22} + X_{22}^T & X_{23} \\ * & * & X_{33} \end{bmatrix},$$
$$R = \begin{bmatrix} R_{11} & R_{12} \\ * & R_{22} \end{bmatrix}, U = \begin{bmatrix} U_{11} & U_{12} \\ * & U_{22} \end{bmatrix}$$

Using Lemma 1, the following inequality is obtained:

$$\begin{aligned} V_1(t) &\geq x(t)^T P x(t) + d(t)\varsigma(t)^T X \varsigma(t) + \tfrac{d(t)}{d}[x(t) - x(t_k)]^T Q [x(t) - x(t_k)] \\ &= \tfrac{d(t)}{d}\varsigma^T(t)\Psi_1^{ij}\varsigma(t) \end{aligned} \quad (22)$$

From LMI (18), $V_1(t) \geq 0$ can be guaranteed, which means that $V(t) \geq 0$.
Taking the derivative of $V(t)$ yields

$$\begin{aligned} \dot{V}_1(t) &= 2\dot{x}(t)^T P x(t) + 2d(t)\varsigma^T(t) X \begin{bmatrix} \dot{x}^T(t) & 0 & x^T(t) \end{bmatrix}^T \\ &\quad -\varsigma^T(t) X \varsigma(t) + d(t)\dot{x}^T(t) Q \dot{x}(t) - \int_{t_k}^{t} \dot{x}^T(s) Q \dot{x}(s) ds, \\ \dot{V}_2(t) &= d(t)\begin{bmatrix} \dot{x}(t) \\ x(t_k) \end{bmatrix}^T R \begin{bmatrix} \dot{x}(t) \\ x(t_k) \end{bmatrix} - \int_{k}^{t} \begin{bmatrix} \dot{x}(s) \\ x(t_k) \end{bmatrix}^T R \begin{bmatrix} \dot{x}(s) \\ x(t_k) \end{bmatrix} ds, \\ \dot{V}_3(t) &= d(t)\begin{bmatrix} x(t_k) \\ x(t) \end{bmatrix}^T U \begin{bmatrix} x(t_k) \\ x(t) \end{bmatrix} - \int_{t_k}^{t} \begin{bmatrix} x(t_k) \\ x(s) \end{bmatrix}^T U \begin{bmatrix} x(t_k) \\ x(s) \end{bmatrix} ds \\ &= d(t)\begin{bmatrix} x(t_k) \\ x(t) \end{bmatrix}^T U \begin{bmatrix} x(t_k) \\ x(t) \end{bmatrix} - \tau(t) x^T(t_k) U_{11} x(t_k) \\ &= -2x^T(t_k) U_{12} \int_{t_k}^{t} x(s) ds - \int_{t_k}^{t} x^T(s) U_{22} x(s) ds \end{aligned}$$

$$\begin{aligned} \dot{V}_4(t) &= d(t)\tau(t)\dot{x}^T(t) Z \dot{x}(t) - d(t)\int_{t_k}^{t} \dot{x}^T(s) Z \dot{x}(s) ds - \int_{-\tau(t)}^{0}\int_{t+\alpha}^{t} \dot{x}^T(s) Z \dot{x}(s) ds d\alpha \\ &\leq \tfrac{(d(t)+\tau(t))^2}{4}\dot{x}^T(t) Z \dot{x}(t) - d(t)\int_{t_k}^{t} \dot{x}^T(s) Z \dot{x}(s) ds - \int_{-\tau(t)}^{0}\int_{t+\alpha}^{t} \dot{x}^T(s) Z \dot{x}(s) ds d\alpha \\ &\leq \tfrac{d}{4} d(t)\dot{x}^T(t) Z \dot{x}(t) + \tfrac{d}{4}\tau(t)\dot{x}^T(t) Z \dot{x}(t) - \tfrac{d(t)}{d}\begin{bmatrix} x(t_k) \\ x(t) \end{bmatrix}^T \begin{bmatrix} Z & -Z \\ -Z & Z \end{bmatrix} \begin{bmatrix} x(t_k) \\ x(t) \end{bmatrix} \\ &\quad -\int_{-\tau(t)}^{0}\int_{t+\alpha}^{t} \dot{x}^T(s) Z \dot{x}(s) ds d\alpha \end{aligned} \quad (23)$$

□

3.2. Introduction of Fuzzy Framework

Using Lemma 1, it can be obtained that

$$
\begin{aligned}
0 &= 2\sum_{i=1}^{r}\sum_{j=1}^{r}\mu_i(z(t))\mu_j(z(t_k))\xi^T(t)N_{ij}\times[\tau(t)x(t)-\int_{t_k}^{t}x(s)ds-\int_{-\tau(t)}^{0}\int_{t+\alpha}^{t}\dot{x}(s)dsd\alpha] \\
&\le 2\tau(t)\sum_{i=1}^{r}\sum_{j=1}^{r}\mu_i(z(t))\mu_j(z(t_k))\xi^T(t)N_{ij}x(t) \\
&-2\sum_{i=1}^{r}\sum_{j=1}^{r}\mu_i(z(t))\mu_j(z(t_k))\xi^T(t)N_{ij}\int_{t_k}^{t}x(s)ds \\
&+\frac{\tau^2(t)}{2}\sum_{i=1}^{r}\sum_{j=1}^{r}\mu_i(z(t))\mu_j(z(t_k))\xi^T(t)N_{ij}Z^{-1}N_{ij}^T\xi(t) \\
&+\frac{2}{\tau^2(t)}\left[\int_{-\tau(t)}^{0}\int_{t+\alpha}^{t}\dot{x}^T(s)dsd\alpha\right]Z\left[\int_{-\tau(t)}^{0}\int_{t+\alpha}^{t}\dot{x}(s)dsd\alpha\right] \\
&\le 2\tau(t)\sum_{i=1}^{r}\sum_{j=1}^{r}\mu_i(z(t))\mu_j(z(t_k))\xi^T(t)N_{ij}x(t) \\
&-2\sum_{i=1}^{r}\sum_{j=1}^{r}\mu_i(z(t))\mu_j(z(t_k))\xi^T(t)N_{ij}\int_{t_k}^{t}x(s)ds \\
&+\frac{\tau^2(t)}{2}\sum_{i=1}^{r}\sum_{j=1}^{r}\mu_i(z(t))\mu_j(z(t_k))\xi^T(t)N_{ij}Z^{-1}N_{ij}^T\xi(t) \\
&+\int_{-\tau(t)}^{0}\int_{t+\alpha}^{t}\dot{x}^T(s)Z\dot{x}(s)dsd\alpha
\end{aligned} \tag{24}
$$

which implies

$$
\begin{aligned}
\int_{-\tau(t)}^{0}\int_{t+\alpha}^{t}\dot{x}(s)Z\dot{x}(s)dsd\alpha \le \sum_{i=1}^{3}\sum_{j=1}^{3}\mu_i(z(t))\mu_j(z(t_k)) \\
\Big[2\tau(t)\xi^T(t)N_{ij}x(t)-2\xi^T(t)N_{ij}\int_{t_k}^{t}x(s)ds \\
+\frac{d\tau(t)}{2}\xi^T(t)N_{ij}Z^{-1}N_{ij}^T\xi(t)\Big]
\end{aligned} \tag{25}
$$

Combine (23) with (25) such that

$$
\begin{aligned}
\dot{V}_4(t) \quad &\le \frac{d}{4}d(t)\dot{x}^T(t)Z\dot{x}(t)+\frac{d}{4}\tau(t)\dot{x}^T(t)Z\dot{x}(t)-\frac{d(t)}{d}\begin{bmatrix} x(t_k) \\ x(t)\end{bmatrix}^T\begin{bmatrix} Z & -Z \\ -Z & Z\end{bmatrix}\begin{bmatrix} x(t_k) \\ x(t)\end{bmatrix} \\
&+\sum_{i=1}^{3}\sum_{j=1}^{3}\mu_i(z(t))\mu_j(z(t_k))\big[2\tau(t)\xi^T(t)N_{ij}x(t) \\
&-2\xi^T(t)N_{ij}\int_{t_k}^{t}x(s)ds+\frac{d\tau(t)}{2}\xi^T(t)N_{ij}Z^{-1}N_{ij}^T\xi(t)\Big]
\end{aligned} \tag{26}
$$

For any matrixes G,$M_{ij}, i, j \in L$ and scalars $\varepsilon_i, i = 1, 2, 3, 4$, we have

$$
0=\sum_{i=1}^{3}\sum_{j=1}^{3}\mu_i(z(t))\mu_j(z(t_k))\xi^T(t)M_{ij}\times\left[x(t)-x(t_k)-\int_{t_k}^{t}\dot{x}(s)ds\right] \tag{27}
$$

$$
\begin{aligned}
0 &= 2\Big[\varepsilon_1 x^T(t)G+\varepsilon_2\dot{x}^T(t)G+\varepsilon_3 x(t_k)G+\varepsilon_4\int_{t_k}^{t}x^T(s)Gds\Big] \\
&\times\left[-\dot{x}(t)+\sum_{i=1}^{3}\sum_{j=1}^{3}\mu_i(z(t))\mu_j(z(t_k))\big(A_i x(t)+B_i K_j x(t_k)\big)\right]
\end{aligned} \tag{28}
$$

From (22), (23) and (26)–(28), we obtain that

$$\begin{aligned} \dot{V}(t) \le \tfrac{d(t)}{d}\sum_{i=1}^{3}\sum_{j=1}^{3}\mu_i(z(t))\mu_j(z(t_k))\xi^T(t)\Psi_3^{ij}\xi(t) \\ +\tfrac{1}{d}\sum_{i=1}^{3}\sum_{j=1}^{3}\mu_i(z(t))\mu_j(z(t_k))\int_{t_k}^{t}\begin{bmatrix}\xi(t)\\ \dot{x}(s)\end{bmatrix}^T\hat{\Psi}_4^{ij}\begin{bmatrix}\xi(t)\\ \dot{x}(s)\end{bmatrix}ds \end{aligned} \tag{29}$$

where

$$\begin{aligned} \hat{\Psi}_4^{ij} &= \begin{bmatrix}\Pi_{11ij} & \Theta_{ij}\\ * & -dQ-R_{11}\end{bmatrix} + \tfrac{d^2}{2}\begin{bmatrix}N_{ij}\\ 0\end{bmatrix}Z^{-1}\begin{bmatrix}N_{ij}\\ 0\end{bmatrix}^T \\ \Theta_{ij} &= \begin{bmatrix}-dM_{1ij}^T & -dM_{2ij}^T & -dR_{12}-dM_{3ij}^T & -dM_{4ij}^T\end{bmatrix}^T \end{aligned} \tag{30}$$

Following the Schur complement, (30) implies $\hat{\Psi}_4^{ij} < 0$. It can be referred that $\dot{V}(t) < -\sigma\| x(t) \|^2$ when
$x(t) \neq 0, \sigma > 0$, which shows that the system (11) is asymptotically stable. This proof is completed.

Remark 2. *To fully capture the available characteristics of sampling patterns, some novel terms, liked* $(t)\int_{-d(t)}^{0}\int_{t+\theta}^{t}\dot{x}(s)^T Z\dot{x}(s)dsd\theta$*, have been introduced in the LKF, which means that the constructed LKF is general.*

Remark 3. *Compared with the LKF in [38,39], more available matrices, such as* Q, R, X, U*, are effectively used in the LKF. If we let* $R_{12} = R_{22} = Z = Q = 0$ *and* $U_{13} = U_{12} = U_{22} = X_{13} = X_{23} = X_{33} = 0$*, the LKF will be reduced to those in [38,39], which means that the proposed LKF has a more general form. Moreover, free matrices* M_{ij} *and* N_{ij} *are introduced into the differentiation of the LKF. Hence, model transformation and bounding techniques are avoided, which overcomes an important source of conservatism.*

Remark 4. *In the process of derivative and further proof of the LKF in [38,39], the positive definite requirement of the matrix is necessary. In this paper, X-dependent terms are introduced in* $V_1(t)$ *and are not required to be positive definite, which means that the limitation conditions of the matrices are overcome. Hence, the conservativeness can be further reduced.*

3.3. Design of Sampled-Data Controller

Theorem 2. *Given scalars* $d > 0$ *and* $\varepsilon_i, i = 1,2,3,4$*, the system (15) is asymptotically stable, if there exist symmetric matrices* $P > 0,\ Q > 0,\ Z > 0,\ \begin{bmatrix}R_{11} & R_{12}\\ * & R_{22}\end{bmatrix} > 0,\ \begin{bmatrix}U_{11} & U_{12}\\ * & U_{22}\end{bmatrix} > 0, X_{11}, X_{13}, X_{22}, X_{23}, X_{33}, G, M_{ij} = \begin{bmatrix}M_{1ij}^T & M_{2ij}^T & M_{3ij}^T & M_{4ij}^T\end{bmatrix}^T, N_{ij} = \begin{bmatrix}N_{1ij}^T & N_{2ij}^T & N_{3ij}^T & N_{4ij}^T\end{bmatrix}^T$*, such that*

$$\Psi_1^{ij} = \begin{bmatrix}P + d\left(X_{11}+X_{11}^T+Q\right) & d\left(X_{11}+X_{22}-Q\right) & dX_{13}\\ * & d\left(X_{11}+X_{22}^T+Q\right) & dX_{23}\\ * & * & dX_{33}\end{bmatrix} > 0 \tag{31}$$

$$\tilde{\Psi}_2^{ij} = \begin{bmatrix}\tilde{\Xi}_{11}^{ij}+\tilde{\Omega}_{11}^{ij} & \tilde{\Xi}_{12}^{ij}+\tilde{\Omega}_{12}^{ij} & \tilde{\Xi}_{13}^{ij}+\tilde{\Omega}_{13}^{ij} & \tilde{\Xi}_{14}^{ij}+dX_{33}^T\\ * & \tilde{\Xi}_{22}^{ij}+\tilde{\Omega}_{22}^{ij} & \tilde{\Xi}_{23}^{ij}+\tilde{\Omega}_{23}^{ij} & \tilde{\Xi}_{24}^{ij}+dX_{13}\\ * & * & \tilde{\Xi}_{33}^{ij}+\tilde{\Omega}_{33}^{ij} & \tilde{\Xi}_{34}^{ij}\\ * & * & * & \tilde{\Xi}_{44}^{ij}\end{bmatrix} < 0 \tag{32}$$

$$\Psi_3^{ij} = \begin{bmatrix}\tilde{\Pi}_{11ij} & \tilde{\Pi}_{12ij}\\ * & \tilde{\Pi}_{22}\end{bmatrix} < 0, \tag{33}$$

where

$$\widetilde{\Pi}_{11ij} = \begin{bmatrix} \widetilde{\Xi}_{11}^{ij} + \widetilde{\Omega}_{11}^{ij} & \widetilde{\Xi}_{12}^{ij} + d\widetilde{N}_{2ij}^{T} & \widetilde{\Xi}_{13}^{ij} + d\widetilde{N}_{3ij}^{T} & \widetilde{\Xi}_{14}^{ij} + d\widetilde{N}_{4ij}^{T} \\ * & \widetilde{\Xi}_{22}^{ij} + \frac{d^2}{4}\widetilde{Z} & \widetilde{\Xi}_{23}^{ij} & \widetilde{\Xi}_{24}^{ij} \\ * & * & \widetilde{\Xi}_{33}^{ij} + \widetilde{\Omega}_{33}^{ij} & \widetilde{\Xi}_{34}^{ij} \\ * & * & * & \widetilde{\Xi}_{44}^{ij} \end{bmatrix},$$

$$\widetilde{\Pi}_{12ij} = \begin{bmatrix} -d\widetilde{M}_{1ij} & d\widetilde{N}_{1ij} \\ -d\widetilde{M}_{2ij} & d\widetilde{N}_{2ij} \\ -d\widetilde{R}_{12}^{T} - d\widetilde{M}_{3ij} & d\widetilde{N}_{3ij} \\ -d\widetilde{M}_{4ij} & d\widetilde{N}_{4ij} \end{bmatrix}, \widetilde{\Pi}_{22} = \begin{bmatrix} -d\widetilde{Q} - d\widetilde{R}_{11} & 0 \\ * & -2\widetilde{Z} \end{bmatrix},$$

$$\widetilde{\Xi}_{11}^{ij} = -\widetilde{X}_{11i} - \widetilde{X}_{11i}^{T} + \widetilde{M}_{1ij}^{T} + \widetilde{M}_{1ij} - \varepsilon_1 A_i \widetilde{G}^{T} - \varepsilon_1 \widetilde{G} A_i^{T}$$

$$\widetilde{\Xi}_{12}^{ij} = P + \widetilde{M}_{2ij}^{T} + \varepsilon_1 \widetilde{G} - \varepsilon_2 A_i^{T} \widetilde{G}^{T}$$

$$\widetilde{\Xi}_{13}^{ij} = \widetilde{X}_{11i} + \widetilde{X}_{22i} + \widetilde{M}_{3ij}^{T} - \widetilde{M}_{1ij} - \varepsilon_1 B_i \widetilde{K}_j - \varepsilon_3 \widetilde{G} A_i^{T}$$

$$\widetilde{\Xi}_{14}^{ij} = -\widetilde{X}_{13i} + \widetilde{M}_{4ij}^{T} - \widetilde{N}_{1ij} - \varepsilon_4 \widetilde{G} A_i^{T}$$

$$\widetilde{\Xi}_{22}^{ij} = \varepsilon_2 \widetilde{G} + \varepsilon_2 \widetilde{G}^{T}$$

$$\widetilde{\Xi}_{23}^{ij} = -\widetilde{M}_{2ij} - B_i \widetilde{K}_j + \varepsilon_3 \widetilde{G}$$

$$\widetilde{\Xi}_{24}^{ij} = \varepsilon_4 \widetilde{G}^{T} - \widetilde{N}_{2ij}$$

$$\widetilde{\Xi}_{33}^{ij} = -\widetilde{X}_{22i} - \widetilde{X}_{22i}^{T} - \widetilde{M}_{3ij}^{T} - \widetilde{M}_{3ij} - \varepsilon_3 B_i \widetilde{K}_j - \varepsilon_3 \widetilde{K}_j^{T} B_i^{T}$$

$$\widetilde{\Xi}_{34}^{ij} = -\widetilde{X}_{23i} - \widetilde{U}_{12} - \widetilde{M}_{4ij}^{T} - N_{3ij} - \varepsilon_4 \widetilde{K}_j^{T} B_i^{T}$$

$$\widetilde{\Xi}_{44}^{ij} = -\widetilde{X}_{33i} - \frac{1}{d}\widetilde{U}_{22} - \widetilde{N}_{4ij}^{T} - \widetilde{N}_{4ij}$$

$$\widetilde{\Omega}_{11} = d\left(\widetilde{X}_{13} + \widetilde{X}_{13}^{T}\right) + d\widetilde{U}_{22} - \widetilde{Z}$$

$$\widetilde{\Omega}_{12} = d\widetilde{X}_{11} + d\widetilde{X}_{11}^{T}$$

$$\widetilde{\Omega}_{13} = d\widetilde{X}_{23}^{T} + d\widetilde{U}_{12}^{T} + \widetilde{Z}$$

$$\widetilde{\Omega}_{22} = d\widetilde{R}_{11} + d\widetilde{Q} + \frac{d^2}{4}\widetilde{Z}$$

$$\widetilde{\Omega}_{23} = -d\left(\widetilde{X}_{11} + \widetilde{X}_{22}\right) + d\widetilde{R}_{12}$$

$$\widetilde{\Omega}_{33} = d\widetilde{R}_{22} + d\widetilde{U}_{11} - \widetilde{Z}$$

The fuzzy controller is obtained that

$$K_j = \widetilde{K}_j \widetilde{G}^{-T} \quad (34)$$

Proof. Denoting

$$\begin{aligned} &\widetilde{G} = G^{-1},\ \widetilde{K}_j = K_j \widetilde{G}^{T},\ \widetilde{P}_i = \widetilde{G} P_i \widetilde{G}^{T},\ \widetilde{X}_{11i} = \widetilde{G} X_{11} \widetilde{G}^{T}, \\ &\widetilde{X}_{22i} = \widetilde{G} X_{22} \widetilde{G}^{T}, \widetilde{X}_{13i} = \widetilde{G} X_{13i} \widetilde{G}^{T}, \widetilde{X}_{23i} = \widetilde{G} X_{23i} \widetilde{G}^{T}, \\ &\widetilde{X}_{33i} = \widetilde{G} X_{33i} \widetilde{G}^{T}, \widetilde{R}_{11} = \widetilde{G} R_{11} \widetilde{G}^{T}, \widetilde{R}_{12} = \widetilde{G} R_{12} \widetilde{G}^{T}, \\ &\widetilde{R}_{22} = \widetilde{G} R_{22} \widetilde{G}^{T}, \widetilde{Q} = \widetilde{G} Q \widetilde{G}^{T}, \widetilde{U}_{11} = \widetilde{G} U_{11} \widetilde{G}^{T}, \widetilde{U}_{12} = \widetilde{G} U_{12} \widetilde{G}^{T}, \\ &\widetilde{U}_{22} = \widetilde{G} U_{22} \widetilde{G}^{T}, \widetilde{Z} = \widetilde{G} Z \widetilde{G}^{T}, \Gamma_1 = diag\left\{\widetilde{G}, \widetilde{G}, \widetilde{G}\right\}, \\ &\Gamma_2 = diag\left\{\widetilde{G}, \widetilde{G}, \widetilde{G}, \widetilde{G}\right\}, \Gamma_3 = diag\left\{\widetilde{G}, \widetilde{G}, \widetilde{G}, \widetilde{G}, \widetilde{G}, \widetilde{G}\right\}, \\ &\widetilde{M}_{ij} = \Gamma_2 M_{ij} \Gamma_2^{T}, \widetilde{N}_{ij} = \Gamma_2 N_{ij} \Gamma_2^{T}. \end{aligned}$$

Pre- and post-multiplying (18), (19), (20) by $\Gamma_1, \Gamma_2, \Gamma_3$ and $\Gamma_1^T, \Gamma_2^T, \Gamma_3^T$, respectively, (31), (32), (33) are obtained. This completed the proof. □

4. Numerical Examples

In this section, an application example of a DPS is introduced to show the superiority of the methods. M, D and G are considered as follows [41].

$$M = \begin{bmatrix} 1.0852 & 0 & 0 \\ 0 & 2.0575 & -0.4087 \\ 0 & -0.4087 & 0.2153 \\ & & \end{bmatrix}, D = \begin{bmatrix} 0.0865 & 0 & 0 \\ 0 & 0.0762 & 0.1510 \\ 0 & 0.0151 & 0.0031 \end{bmatrix},$$

$$G = \begin{bmatrix} 0.0389 & 0 & 0 \\ 0 & 0.0266 & 0 \\ 0 & 0 & 0 \end{bmatrix}.$$

Let $\alpha = \sin 2^0$ and $\beta = \cos 88^0$, we have

$$A_1 = \begin{bmatrix} 0 & 0 & 0 & 1.0000 & -0.0349 & 0 \\ 0 & 0 & 0 & 0.0349 & 1.0000 & 0 \\ 0 & 0 & 0 & 0 & 0 & 1.0000 \\ -0.0358 & 0 & 0 & -0.0797 & 0 & 0 \\ 0 & -0.0208 & 0 & 0 & -0.0818 & -0.1224 \\ 0 & -0.0394 & 0 & 0 & -0.2254 & -0.2468 \end{bmatrix},$$

$$A_2 = \begin{bmatrix} 0 & 0 & 0 & 0.0349 & -1.0000 & 0 \\ 0 & 0 & 0 & 1.0000 & 0.0349 & 0 \\ 0 & 0 & 0 & 0 & 0 & 1.0000 \\ -0.0358 & 0 & 0 & -0.0797 & 0 & 0 \\ 0 & -0.0208 & 0 & 0 & -0.0818 & -0.1224 \\ 0 & -0.0394 & 0 & 0 & -0.2254 & -0.2468 \end{bmatrix},$$

$$A_3 = \begin{bmatrix} 0 & 0 & 0 & 0.0349 & 1.0000 & 0 \\ 0 & 0 & 0 & -1.0000 & 0.0349 & 0 \\ 0 & 0 & 0 & 0 & 0 & 1.0000 \\ -0.0358 & 0 & 0 & -0.0797 & 0 & 0 \\ 0 & -0.0208 & 0 & 0 & -0.0818 & -0.1224 \\ 0 & -0.0394 & 0 & 0 & -0.2254 & -0.2468 \end{bmatrix},$$

$$B_i = \begin{bmatrix} 0 & 0 & 0 \\ 0 & 0 & 0 \\ 0 & 0 & 0 \\ 0.9215 & 0 & 0 \\ 0 & 0.7802 & 1.4811 \\ 0 & 1.4811 & 7.4562 \end{bmatrix}, \ i = 1,2,3.$$

Firstly, we compare the proposed method with references that used traditional T-S fuzzy models. From Table 1, the maximum sampling internal is $d = 0.681$. Note that results in [37–39] are 0.25, 0.264, and 0.532, respectively. This means that the sampling internal in this paper improves [37–39] by 160.8, 146.97, and 22.56%, respectively. It also shows that the proposed controllers play an important role in obtaining a longer sampling interval.

Table 1. Maximum values of the upper sampling internal.

Method	[37]	[38]	[39]	Theorem 1
d_2	0.25	0.264	0.532	0.681

Next, we combined references that used different methods, such as T-set [42], Pareto optimality under T-set [43], and intuitionistic fuzzy T-set [44], to obtain the maximum sampling internal. In Table 2, we can see that the values of the obtained sampling internal were close to the method proposed in this paper, which illustrates that the technology derived from the T-set has its advantages. And T-sets can be used to replace fuzzy sets to represent uncertainty.

Table 2. Maximum values of the upper sampling internal.

Technologies	Maximum Sampling Internal
T-set	0.583
Pareto optimality under T-set	0.624
Intuitionistic fuzzy T-set	0.652
Proposed method	0.681

The initial values are chosen that $x_s(t) = \begin{bmatrix} 15\text{ m} & 15\text{ m} & 0.2^\circ & 0\text{ m/s} & 0\text{ m/s} & 0^\circ \end{bmatrix}$.
And the other parameters are $d = 1.6\text{s}, \varepsilon_1 = \varepsilon_2 = 1, \varepsilon_3 = \varepsilon_4 = 0$. Then, the gain can be computed that

$$K_1 = \begin{bmatrix} -0.0260 & -0.0387 & -0.0309 & -0.6802 & -0.0002 & -0.0004 \\ 0.0619 & -0.0067 & 0.0395 & 0.0004 & -1.3157 & 0.2556 \\ -0.0124 & 0.0061 & 0.0066 & -0.0001 & 0.2653 & -0.1315 \end{bmatrix}$$

$$K_2 = \begin{bmatrix} -0.0123 & 0.0143 & 0.0154 & -0.7071 & -0.0002 & 0.0000 \\ -0.0196 & 0.0251 & 0.0698 & 0.0003 & -1.3667 & 0.2643 \\ 0.0041 & -0.0002 & 0.0011 & -0.0001 & 0.2754 & -0.1364 \end{bmatrix}$$

$$K_3 = \begin{bmatrix} -0.0123 & 0.0143 & 0.0154 & -0.7071 & -0.0002 & 0.0000 \\ -0.0196 & 0.0251 & 0.0698 & 0.0003 & -1.3667 & 0.2643 \\ 0.0041 & -0.0002 & 0.0011 & -0.0001 & 0.2754 & -0.1364 \end{bmatrix}$$

To illustrate the control performance of the proposed approaches, comparison results with those of the PID controller [45] are presented in Figures 4–9.

The PID value was chosen such that

$$K_p = diag\left([2.8 \times 10^3, 6 \times 10^3, 2.3 \times 10^6]\right)$$
$$K_p = diag\left([1, 1, 1]\right)$$
$$K_p = diag\left([4.5 \times 10^4, 3.5 \times 10^4.1 \times 10^4]\right)$$

In Figures 4–9 it is shown that the ship's position, yaw angle, and velocities reached expected values within about 10 s, while under the PID controller designed in [39], it took longer to reach the predetermined targets, which means that the designed method in this paper, which used the proposed method, has a faster response speed. In addition, this demonstrates that the oscillation amplitude of the system is relatively small, indicating that the designed controllers have good anti-interference ability. Meanwhile, Figures 4–9 further indicate that the designed sampled-data controller also has a relatively fast speed response time, which means that the controller has fast convergence speed and high stability.

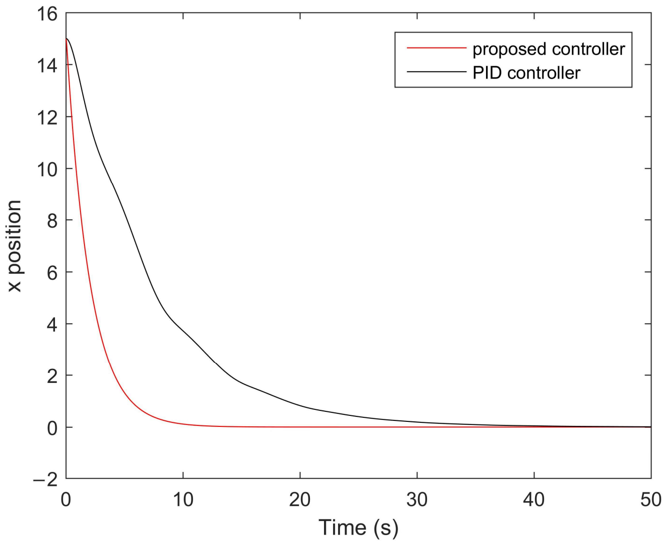

Figure 4. The x position compared with that of the PID controller.

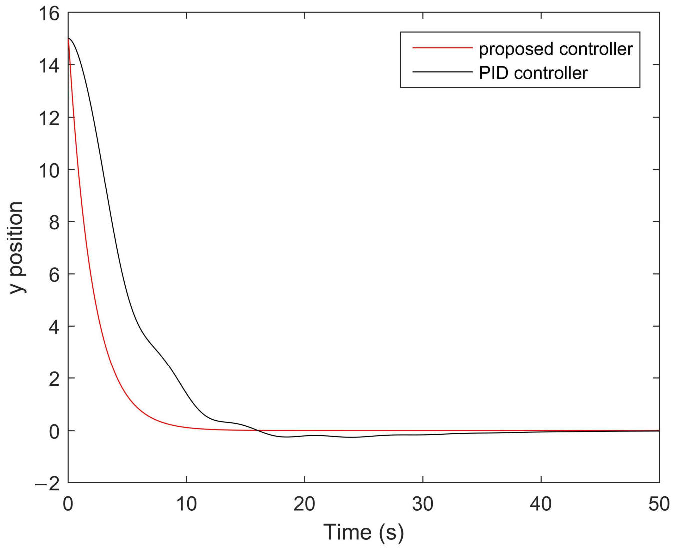

Figure 5. The y position compared with that of the PID controller.

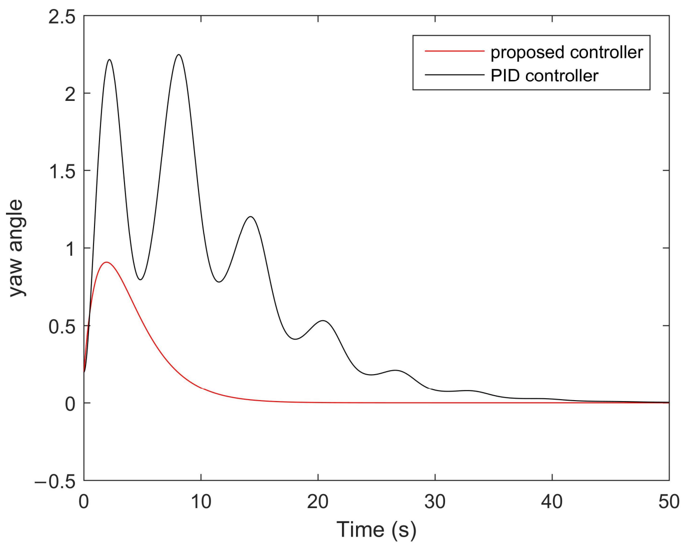

Figure 6. Yaw angle compared with that of the PID controller.

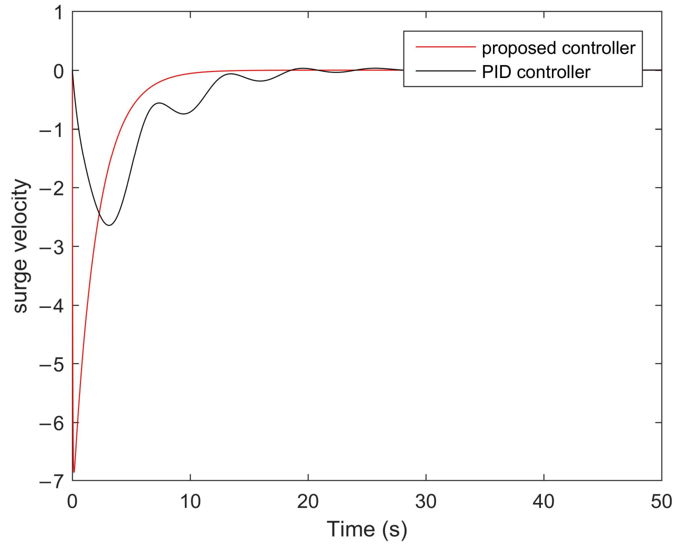

Figure 7. Surge velocity compared with that of the PID controller.

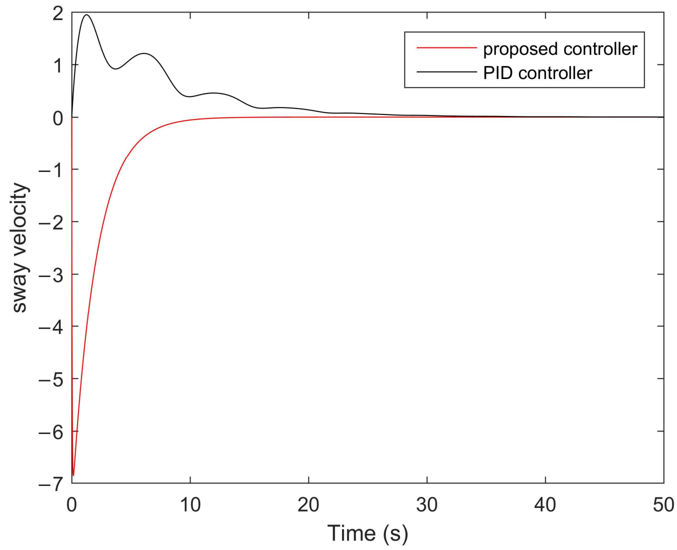

Figure 8. Sway velocity compared with that of the PID controller.

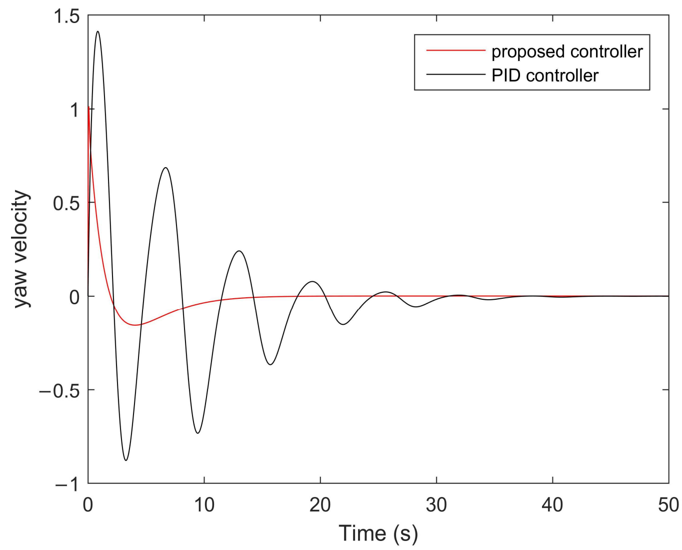

Figure 9. Yaw velocity compared with that of the PID controller.

5. Conclusions

This article investigated DPS stabilization problems using sampled-data under T-S fuzzy models. To reduce the conservatism of the obtained results, some novel terms were introduced in the constructed LKF, and a larger sampling interval was achieved. The main novelty of the LKF is that the sampling mode information is fully utilized; in addition, the positive definite constraints of LKFs are relaxed, and additional free matrices are provided to further reduce the conservatism. Experimental results showed that the developed control methods are superior. In the future, we will explore using the T-set method instead of the fuzzy set to represent real-life scenarios and fully consider the characteristics of linear time-varying systems [46], which will become a new topic in future work.

Author Contributions: Writing—original draft preparation, M.Z.; software, Y.S.; writing—review and editing, C.Y. All authors have read and agreed to the published version of the manuscript.

Funding: This study was funded by the National Natural Science Foundation of China (No. 52371369), the Key Projects of the National Key R & D Program (No. 2021YFB390150), the National Science Project of Fujian Province (Nos. 2022J01323, 2021J01822, 2020J01660, 2020J01659 and 2023J01325), and the Fuzhou-Xiamen-Quanzhou Independent Innovation Region Cooperated Special Foundation (No. 3502ZCQXT2021007).

Data Availability Statement: Data are contained within the article.

Conflicts of Interest: The authors declare no conflicts of interest.

References

1. Fossen, T.I. *Guidance and Control of Ocean Vehicles*; Wiley: New York, NY, USA, 1994.
2. Wang, Y.L.; Han, Q.L.; Fei, M.R.; Peng, C. Network-based T-S fuzzy dynamic positioning controller design for unmanned marine vehicles. *IEEE Trans. Cybern.* **2018**, *48*, 2750–2763. [CrossRef]
3. Hao, L.Y.; Zhang, H.; Li, T.S.; Lin, B.; Chen, C.P. Fault tolerant control for dynamic positioning of unmanned marine vehicles based on T-S fuzzy model with unknown membership functions. *IEEE Trans. Veh. Technol.* **2021**, *70*, 146–157. [CrossRef]
4. Veksler, A.; Johansen, T.A.; Borrelli, F.; Realfsen, B. Dynamic positioning with model predictive control. *IEEE Trans. Control Syst. Technol.* **2016**, *24*, 1340–1353. [CrossRef]
5. Nguyen, V.S. Investigation of a multitasking system for automatic ship berthing in marine practice based on an integrated neural controller. *Mathematics* **2020**, *8*, 1167. [CrossRef]
6. Benetazzo, F.; Ippoliti, G.; Longhi, S.; Raspa, P. Advanced control for fault-tolerant dynamic positioning of an offshore supply vessel. *Ocean Eng.* **2015**, *106*, 472–484. [CrossRef]
7. Karimi, H.R.; Lu, Y. Guidance and control methodologies for marine vehicles: A survey. *Control Eng. Pract.* **2021**, *111*, 104785. [CrossRef]
8. Wang, Y.; Yang, X.; Yan, H. Reliable fuzzy tracking control of near-space hypersonic vehicle using aperiodic measurement information. *IEEE Trans. Ind. Electron.* **2019**, *66*, 9439–9447. [CrossRef]
9. Karimi, H.R. Robust $H\infty$ filter design for uncertain linear systems over network with network-induced delays and output quantization. *Nor. Foren. Autom.* **2009**, *30*, 27–37. [CrossRef]
10. Kiruthika, R.; Krishnasamy, R.; Lakshmanan, S.; Prakash, M.; Manivannan, A. Non-fragile sampled-data control for synchronization of chaotic fractional-order delayed neural networks via LMI approach. *Chaos Solitons Fractals* **2023**, *169*, 113252. [CrossRef]
11. Wang, Y.; Xia, Y.; Zhou, P. Fuzzy-model-based sampled-data control of chaotic systems: A fuzzy time-dependent Lyapunov–Krasovskii functional approach. *IEEE Trans. Fuzzy Syst.* **2016**, *25*, 1672–1684. [CrossRef]
12. Wang, Y.; Shi, P. On master-slave synchronization of Chaotic Lur'e systems using sampled-data control. *IEEE Trans. Circuits Syst. II Express Briefs* **2016**, *85*, 981–992. [CrossRef]
13. Chen, W.-H.; Wang, Z.; Lu, X. On sampled-data control for masterslave synchronization of chaotic Lur'e systems. *IEEE Trans. Circuits Syst. II Express Briefs* **2012**, *59*, 515–519.
14. Wu, Z.-G.; Shi, P.; Su, H.; Chu, J. Local synchronization of chaotic neural networks with sampled-data and saturating actuators. *IEEE Trans. Cybern.* **2014**, *44*, 2635–2645.
15. Wu, Z.G.; Shi, P.; Su, H.Y. Stochastic Synchronization of Markovian Jump Neural Networks with Time-Varying Delay Using Sampled Data. *IEEE Trans. Cybern.* **2013**, *43*, 796–1806. [CrossRef] [PubMed]
16. Karimi, H.R.; Gao, H. Mixed H2/H∞ output-feedback control of second-order neutral systems with time-varying state and input delays. *ISA Trans.* **2008**, *47*, 311–324. [CrossRef]
17. Wei, Y.; Karimi, H.R.; Yang, S. New results on sampled-data output-feedback control of linear parameter-varying systems. *Int. J. Robust Nonlinear Control* **2022**, *32*, 5070–5085. [CrossRef]
18. Li, S.; Yang, L.; Li, K.; Gao, Z. Robust sampled-data cruise control scheduling of high speed train. *Transp. Res. Part C Emerg. Technol.* **2014**, *46*, 274–283. [CrossRef]

19. Wang, Y.; Wang, Q.; Zhou, P.; Duan, D. Robust H∞ directional control for a sampled-data autonomous airship. *J. Cent. South Univ.* **2014**, *21*, 1339–1346. [CrossRef]
20. Zheng, M.; Zhou, Y.; Yang, S.; Li, L. Robust H∞ control of neutral system for sampled-data dynamic positioning ships. *IMA J. Math. Control Inf.* **2019**, *36*, 1325–1345. [CrossRef]
21. Zou, Z.; Zheng, M. Design and stabilization analysis of luxury cruise with dynamic positioning systems based on sampled-data control. *Math. Biosci. Eng.* **2023**, *20*, 14026–14045. [CrossRef] [PubMed]
22. Zheng, M.; Su, Y.; Yang, S.; Li, L. Reliable fuzzy dynamic positioning tracking controller for unmanned surface vehicles based on aperiodic measurement information. *Int. J. Fuzzy Syst.* **2023**, *25*, 358–368. [CrossRef]
23. Castro, M.F.; Seuret, A.; Leite, V.J.; Silva, L.F. Robust local stabilization of discrete time varying delayed state systems under saturating actuators. *Automatica* **2020**, *122*, 109266. [CrossRef]
24. Ge, G.; Lei, D.; Han, Q. A distributed event-triggered transmission strategy for sampled-data consensus of multi-agent systems. *Automatica* **2014**, *50*, 1489–1496.
25. Zhang, X.; Han, Q.; Zhang, B. An overview and deep investigation on sampled-data-based event-triggered control and filtering for networked systems. *IEEE Trans. Ind. Inform.* **2017**, *13*, 4–16. [CrossRef]
26. Yan, L.; Wang, Z.; Zhang, M.; Fan, Y. Sampled-data control for mean-square exponential stabilization of memristive neural networks under deception attacks. *Chaos Solitons Fractals* **2023**, *174*, 113787. [CrossRef]
27. Yerudkar, A.; Chatzaroulas, E.; Del Vecchio, C.; Moschoyiannis, S. Sampled-data control of probabilistic boolean control networks: A deep reinforcement learning approach. *Inf. Sci.* **2023**, *619*, 374–389. [CrossRef]
28. Wang, Y.; Karimi, H.R.; Lam, H.K.; Shen, H. An improved result on exponential stabilization of sampled-data fuzzy systems. *IEEE Trans. Fuzzy Syst.* **2018**, *26*, 3875–3883. [CrossRef]
29. Yan, S.; Gu, Z.; Park, J.H.; Xie, X. Adaptive memory-event-triggered static output control of T–S fuzzy wind turbine systems. *IEEE Trans. Fuzzy Syst.* **2021**, *30*, 3894–3904. [CrossRef]
30. Cai, X.; Shi, K.; She, K.; Zhong, S.; Tang, Y. Quantized sampled-data control tactic for TS fuzzy NCS under stochastic cyber-attacks and its application to truck-trailer system. *IEEE Trans. Veh. Technol.* **2022**, *71*, 7023–7032. [CrossRef]
31. Wang, Y.; Xia, Y.; Ahn, C.K.; Zhu, Y. Exponential stabilization of takagi–sugeno fuzzy systems with aperiodic sampling: An aperiodic adaptive event-triggered method. *IEEE Trans. Syst. Man Cybern. Syst.* **2019**, *49*, 444–454. [CrossRef]
32. Sheng, Z.; Lin, C.; Chen, B.; Wang, Q.-G. Stability and Stabilization of TS Fuzzy Time-delay Systems under Sampled-data Control via New Asymmetric Functional Method. *IEEE Trans. Fuzzy Syst.* **2023**, *31*, 3197–3209. [CrossRef]
33. Velmurugan, G.; Joo, Y.H. Sampled-Data Control Design for T-S Fuzzy System via Quadratic Function Negative Determination Approach. *IEEE Trans. Fuzzy Syst.* **2023**, *31*, 3197–3209. [CrossRef]
34. Katayama, H. Nonlinear Sampled-Data Stabilization of Dynamically Positioned Ships. *IEEE Trans. Control Syst. Technol.* **2010**, *18*, 463–468. [CrossRef]
35. Katayama, H.; Aoki, H. Straight-line trajectory tracking control for sampled-data underactuated ships. *IEEE Trans. Control Syst. Technol.* **2014**, *22*, 1638–1645.
36. Zheng, M.; Zhou, Y.; Yang, S.; Suo, Y.; Li, L. Robust H∞ Control for Sampled-data Dynamic Positioning Ships. *J. Control Eng. Appl. Inform.* **2017**, *19*, 84–92. [CrossRef]
37. Yang, S.; Zheng, M. H-infinity Fault-Tolerant Control for Dynamic Positioning Ships based on Sampled-data. *J. Control Eng. Appl. Inform.* **2018**, *20*, 32–39.
38. Zheng, M.; Yang, S.; Li, L. Stability analysis and T-S fuzzy dynamic positioning controller design for autonomous surface vehicles based on sampled-data control. *IEEE Access* **2020**, *8*, 148193–148202. [CrossRef]
39. Chen, G.; Suo, Y.; Zheng, M.; Yang, S.; Li, L. Reliable tracking control of dynamic positioning ships based on aperiodic measurement information. *J. Control Eng. Appl. Inform.* **2022**, *24*, 80–89.
40. Sun, J.; Liu, G.P.; Chen, J. Delay-dependent stability and stabilization of neutral time-delay systems. *Int. J. Robust Nonlinear Control* **2009**, *19*, 1364–1375. [CrossRef]
41. Tannuri, E.; Agostinho, A.; Morishita, H.; Moratelli, L. Dynamic positioning systems: An experimental analysis of sliding mode control. *Control Eng. Pract.* **2010**, *18*, 1121–1132. [CrossRef]
42. Garai, A.; Mandal, P.; Roy, T.K. Multipollutant air quality management strategies: T-Sets based optimization technique under imprecise environment. *Int. J. Fuzzy Syst.* **2017**, *19*, 1927–1939. [CrossRef]
43. Garai, A.; Mondal, B.; Roy, T.K. Optimisation of multi-objective commercial bank balance sheet management model: A parametric T-set approach. *Int. J. Math. Oper. Res.* **2019**, *15*, 395–416. [CrossRef]
44. Garai, A.; Mandal, P.; Roy, T.K. Intuitionistic fuzzy T-sets based optimization technique for production-distribution planning in supply chain management. *Opsearch* **2016**, *53*, 950–975. [CrossRef]
45. Hu, X.; Du, J.; Shi, J. Adaptive fuzzy controller design for dynamic positioning system of vessels. *Appl. Ocean Res.* **2015**, *53*, 46–53. [CrossRef]
46. De la Sen, M. Robust stability of a class of linear time-varying systems. *IMA J. Math. Control Inf.* **2002**, *19*, 399–418. [CrossRef]